Diagnostic Imaging of the Canine Stifle: A Review

Dominic J. Marino[1], DVM, Diplomate ACVS & ACCT, CCRP and Catherine A. Loughin[1], DVM, Diplomate ACVS & ACCT

[1]Department of Surgery, Long Island Veterinary Specialists, Plainview, NY

Corresponding Author
Dominic J. Marino, DVM, Diplomate ACVS & ACCT, CCRP Long Island Veterinary Specialists, 163 South Service Road, Plainview, NY 11803
E-mail: bongorno@aol.com

Submitted May 2009
Accepted January 2010

DOI:10.1111/j.1532-950X.2010.00678.x

The stifle joint, a common location for lameness in dogs, is a complex arrangement of osseous, articular, fibrocartilaginous, and ligamentous structures. The small size of its component structures, restricted joint space, and its intricate composition make successful diagnostic imaging a challenge. Different tissue types and their superimposition limit successful diagnostic imaging with a single modality. Most modalities exploit the complexity of tissue types found in the canine stifle joint. Improved understanding of the principles of each imaging modality and the properties of the tissues being examined will enhance successful diagnostic imaging.

Since the discovery of X-rays by Roentgen in 1895, their use in diagnostic imaging techniques has evolved. The digital era with enhanced computer capability has resulted in substantial improvements in image quality with reduced acquisition time. Ultrasonography developed in the1940s uses sound waves and thermal imaging developed in the 1950s uses temperature measurements to generate diagnostic images. Diagnostic magnetic resonance imaging (MRI) reported in 1971[1] uses magnetic resonance rather than ionizing radiation with improved image resolution and patient safety. In the 1990s, multidetector computed tomography (CT) technology allowed for the generation of "stacked" or 3-dimensional (3D) images that could be computer manipulated for presurgical planning. The purpose of this review is to outline the principles of each of modality and to describe the utility of each for imaging the canine stifle joint.

RADIOGRAPHY

Because tissues do not absorb X-rays uniformly, images have regions of white, black, and shades of gray. Soft tissue absorbs fewer X-rays than bone resulting in images that are shades of gray whereas bone appears radiopaque.[2] These properties of energy absorption make radiographs ideal for orthopedic conditions such as those that affecting the stifle and radiography remains the most important initial diagnostic step in determining the cause of disease. Radiographic evidence of disease may include: compression of the infrapatellar fat pad, increased synovial fluid volume or thickening of the synovial lining, altered joint space, decreased or increased subchondral bone opacity, mineralization of soft tissues, intraarticular mineralization, joint displacement, or joint malformation.[2] Standard radiographic projections (mediolateral and craniocaudal) are used to make theses assessments and determine if further diagnostic tests are needed. If the craniocaudal view is not taken with the limb in extension, a normal joint space may appear collapsed leading to misinterpretation.

Osteoarthritis (OA) has many different causes, either primary in geriatric animals or secondary to stresses on the joint.[2–5] Evaluation of the subchondral bone, articular margins, and regions of ligament, tendon, and joint capsule attachment are easily assessed on conventional radiographs.[4] The most common radiographic changes noted with stifle OA include narrowing of the joint space; subchondral sclerosis of the tibial plateau; osteophytosis of the trochlear ridges, patella, fabella, ligament attachments, and caudal tibial plateau; cystic lesions; intraarticular mineralization; bone remodeling; and joint capsule distention identified as proximal displacement of the infrapatellar fat pad and caudal displacement of the capsule. Narrowing of the joint space should be assessed during a weight bearing study; however, it can be evident in dogs with advanced disease.[2–4,6–8]

Cranial cruciate ligament (CCL) rupture is the most common disease of the canine stifle joint. In some dogs it can be difficult to diagnose by palpation for cranial drawer or tibial compression tests.[9–11] Radiographic signs include intraarticular swelling, cranial displacement of the tibia in the mediolateral view with tarsal flexion applied (Cazieux-positive sign), and in chronic cases, OA changes.[3–12] The tibial compression stress radiograph has been reported useful in the diagnosis of partial CCL rupture. This radiographic projection requires the stifle to be in 90° of flexion with manual flexional forces applied to the tarsus. Flexion of the hock joint allows the tibia to move cranially so it can be evaluated with during this stress view.[9–11]

Patellar luxation is also frequently reported in the canine stifle and can easily be diagnosed by palpation of the displaced patella in most cases; however, radiographs

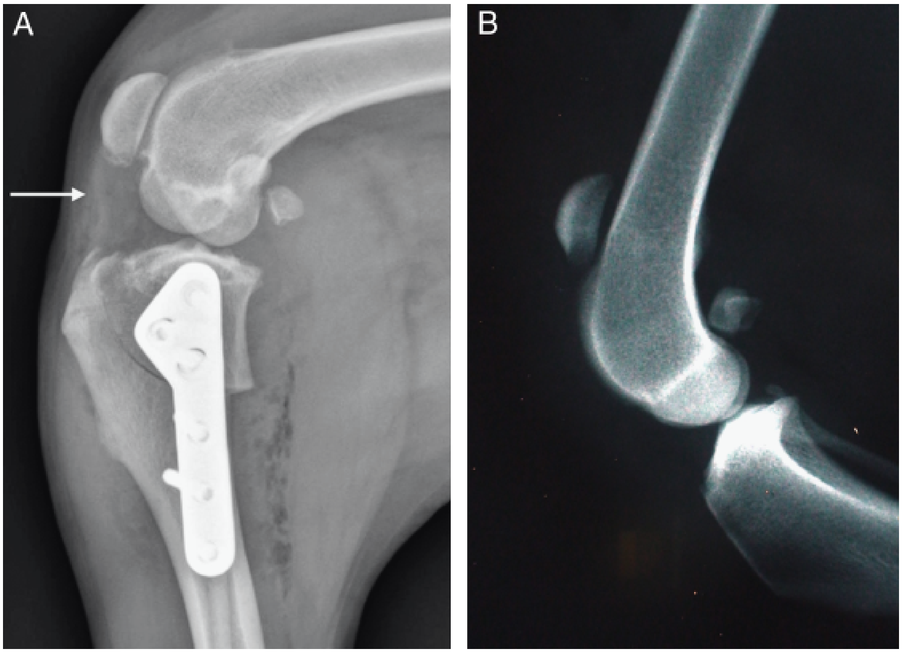

Figure 1 Mediolateral radiographs. (A) A thickened and inflamed patellar tendon (white arrow) 8 weeks after tibial plateau leveling osteotomy. (B) Patellar tendon rupture. Note the proximal position of the patella at the supracondylar region.

may be helpful in assessing alignment of the femur and tibia as well as malformations and rotation.[3,5] Radiographic identification of the patella medial or lateral to the distal aspect of the femur in the craniocaudal view, or superimposed on the femoral condyles in the mediolateral view is diagnostic for patella luxation. A skyline view generated by a cranioproximal 100° craniodistal oblique projection can be used to detect a shallow trochlear groove. The craniocaudal view can be used to demonstrate proximal tibial rotation, coxa vara, femoral or tibial torsion, proximodistal patella alignment, and abnormal angulation of the femorotibial articulation and to quantify any secondary OA.[3,5,13,14] Other patellar abnormalities that can be identified are patellar fractures, thickening of the patellar tendon (Fig 1), and patellar tendon rupture.[15–18]

Osteochondrosis, a disruption of osteochondral ossification resulting in cartilaginous lesions, commonly involves the medial or lateral femoral condyle.[3,5] Radiographic findings include: subchondral bone defect, sclerosis of the defect margins, osteochondral fragments, and secondary OA.[3,5,19] Standard mediolateral and craniocaudal views can be used to demonstrate the defect most often, but a mediolateral oblique view or craniocaudal view with the stifle flexed to an angle of 35–45° may be necessary in some dogs.[3,19]

Neoplasia of the stifle is uncommon and synovial cell sarcoma (Fig 2) is the most common type observed. This tumor arises from the periarticular soft tissues of the stifle and invades the joint and adjacent bone. Standard radiographic views may reveal soft tissue swelling and periosteal proliferation. The most predominant features are multifocal areas of bone destruction in periarticular locations extending into articular regions with possible patella, fabella, tibia, or femur involvement; however, biopsy is needed for confirmation. Other neoplasms include: fibrosarcoma, rhabdomyosarcoma, fibromyxosarcoma, histiocytic sarcoma, liposarcoma, chondrosarcoma, and undifferentiated sarcoma.[2,5] Synovial osteochondromas affecting the stifle are benign and typically well-defined, rounded with multiple calcified intraarticular nodules.[2,3]

Joint fluid analysis and cytology, immune profile, and infectious titers are used in conjunction with radiography to differentiate possible causes of joint infection. Radiographs of stifles with infectious arthritis in the early stages may only reveal soft tissue swelling of the stifle joint. In more advanced cases, subchondral bone erosion and sclerosis, periarticular new bone formation, uneven margins of the joint space, osteolysis and signs of OA are noted. There are many causes of noninfectious arthritis including: rheumatoid arthritis, systemic lupus erythematosus (SLE), feline polyarthritis, and villonodular synovitis, which typically result in soft tissue swelling apparent on radiographic views. Rheumatoid arthritis may also have cyst-like lesions, narrowing of the joint space and regions of lysis. The erosive version of feline polyarthritis is also associated with radiographic subchondral bone defects, whereas radiographic findings of villonodular synovitis is most associated with cortical defects.[2,3,5]Long digital extensor tendon avulsion is frequently associated with mineralization of the tendon, avulsion fragments near the extensor fossa, or as an osseous defect at the fossa.[3,20] Avulsion fractures of the tibial crest can be identified on lateral radiographic projections. Capsular, ligamentous, and tendinous injury can also have distinct radiographic findings including periarticular swelling, avulsion fractures at attachment sites, instability or subluxation, and spatial

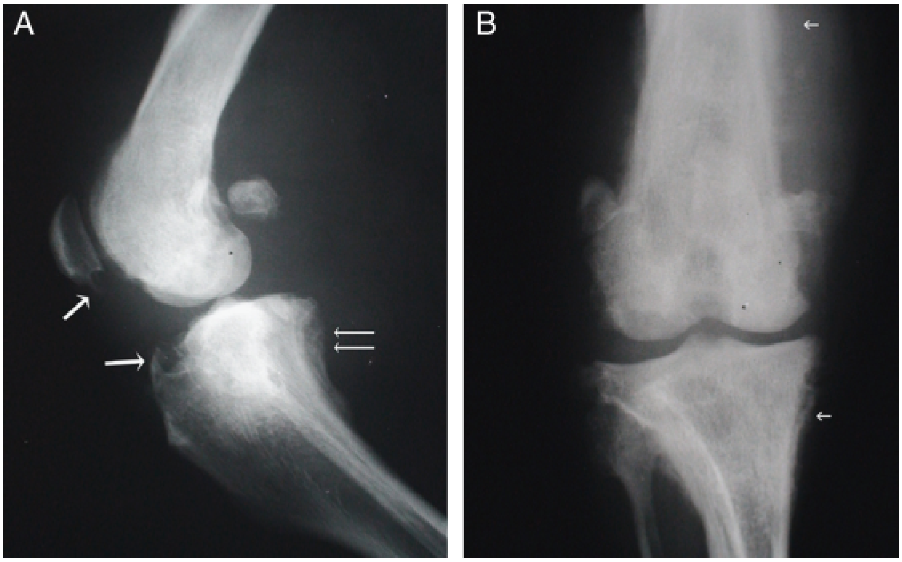

Figure 2 Mediolateral (A) and craniocaudal (B) projections of a stifle with synovial cell sarcoma. Bone lysis is evident on the patella and proximal tibia (single white arrows), and periosteal reaction on the caudal proximal tibia (double white arrow).

derangements. Most of the abnormalities are seen on standard radiographic views, but stress views may be necessary to solidify the diagnosis.[2,3]For most diseases of the stifle, radiography may be sufficient to make a diagnosis when clinical signs and physical examination findings are included in the evaluation; however, if radiographic assessment is inconclusive, more advanced imaging is necessary.

ULTRASONOGRAPHY

When imaging joints, sound waves will travel fastest through bone and slower in joint fluid, making ultrasonography more useful for soft tissue structures of the stifle. Ultrasonography is useful for assessing cartilage abnormalities, meniscal tears, muscle, tendon and ligament abnormalities, arthropathies, and neoplasia. Diagnosis of CCL rupture can be made by demonstration of the fluttering edges of the ruptured ligament (Fig 3). If the infrapatellar fat pad obscures observation of the ruptured CCL, saline solution can be injected into the joint to create an anechoic window.[20–22]

A ruptured patellar tendon appears swollen with irregular margins on ultrasound evaluation and is hyporeflective to hyperreflective. Any bone fragments >3 mm will have acoustic shadowing.[20–23] Thickening of the patellar tendon, as observed in dogs after tibial plateau leveling osteotomy (TPLO), appears as hypoechoic to anechoic centrally with disruption of the normal ligamentous pattern of the fibrils.[17] Patellar luxation and fracture may also be identified with ultrasound.[22] Other conditions of the stifle that can be assessed with ultrasound are OA, osteochondrosis, damaged menisci, collateral ligament damage, neoplasia, and long digital extensor tendon avulsions. OA changes appear as hyperreflective with irregular borders on the bone surface, whereas osteochondrosis is associated with cartilage defects. Free floating cartilage fragments appear hyperreflective.

The entire meniscus is difficult to observe. Normally the meniscus is inhomogeneous and congruent with the margins of the femoral and tibial condyles. Meniscal injury results in hyperreflective with hyporeflective areas that are irregular in shape and displaced. Collateral ligament damage appears hypoechoic to anechoic, and homogeneous to inhomogeneous. Tumors also appear inhomogeneous with irregular borders and are hypoechoic to hyperechoic. Avulsions of the long digital extensor tendon are observed as hyperreflective structures with acoustic shadowing.[20–22,24]

There are substantial limitations to the routine use of ultrasound in evaluating the stifle joint. Small and medium

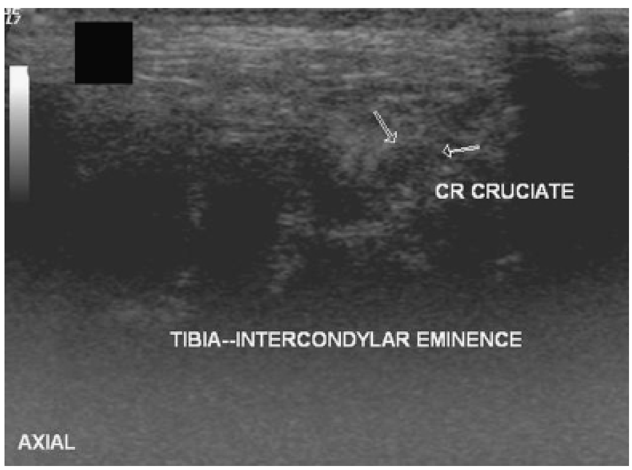

Figure 3 Ultrasound image of a stifle with a ruptured cranial cruciate ligament. The white arrows point to the fluttered edges of the torn ligament.

breed dogs have a narrow stifle resulting in a limited window for image production. Ultrasound images generally have low resolution and soft tissue contrast which may make other imaging modalities such as MRI more useful.[20]

THERMOGRAPHY

Thermography is a noninvasive, diagnostic imaging technique that records cutaneous thermal patterns generated by the infrared emission of surface body heat. These patterns reflect thermal gradients on a color map in which the warmest regions are white or red, and the cooler regions are blue or black. Surface heat measured from the skin is directly related to the local dermal microcirculation, which is under direct control of the sympathetic autonomic nervous system. Conduction of heat from deeper portions of the body to the surface does not occur or create changes in the surface temperature. The clinical basis for thermography is the correlation of temperature recordings with various disease conditions or injury as they relate to autonomic function.[25–28] Thermography can be used as a diagnostic screening tool, as an adjunctive test to enhance physical examination interpretation, to guide therapeutic management, and to assess long term response to treatment.[25–27,29–32] Thermography in dogs has been limited to research applications but is being used clinically in our hospital. [26,33–37]

In an experimentally induced model of canine stifle arthritis, thermographic color maps changed as the temperature increased in the dermatome of the arthritic joints. Acupuncture was used for 4 weeks and the thermographic patterns and temperatures returned to normal whereas thermographic patterns remained abnormal in the untreated group.[33] In studies involving the human knee, researchers consistently find that the patella has a cooler color and temperature whereas the surrounding surface has a warmer color and an increased temperature with synovitis and orthopedic disease.[32,38–46] Similar changes have been observed in equine inflammatory joint disease.[29,31]In experimentally induced calcanean tendon tears in dogs, this same asymmetry and increase in color map and temperature over the injured region were noted.[37]

Thermography has proven beneficial in human and equine medicine. Compared with other imaging modalities it is noninvasive, does not require anesthesia, and does not expose the patient to radiation. Many studies have noted the ability of thermography to detect changes in the thermal pattern before clinical or radiographic signs were identified.[28,30,31,41,47,48] In people, changes in thermographic patterns are associated with different diseases of the knee, making thermography a useful screening test.[38–44,47–49] Development of image recognition software to facilitate computer analysis of thermographic images is being developed. Using image recognition analysis, cranial stifle images were 85% successful for differentiation of normal and CCL ligament deficient stifles in both clipped and

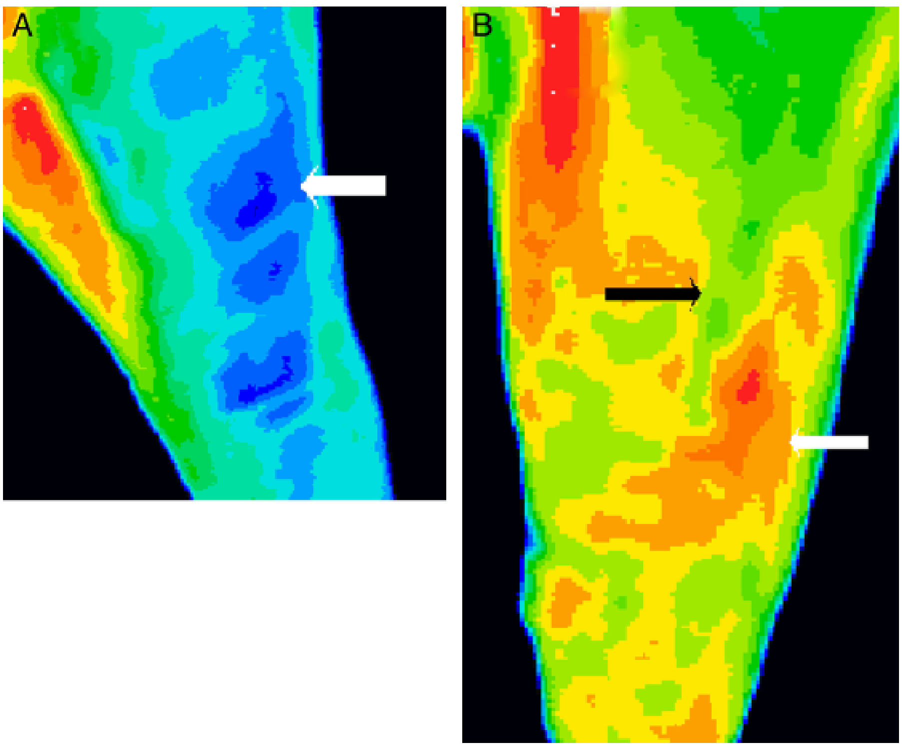

Figure 4 (A) Cranial thermal image of a normal canine stifle. The patella (white arrow) is a cooler color (dark blue) than the rest of the joint (which is warmer (light blue to green). (B) Thermal image of a stifle with a ruptured cranial cruciate ligament. The patella (black solid arrow) is cooler than the inflamed joint (black open arrow).

unclipped dogs (Fig 4). Medial, caudal, and lateral images were 75–85% successful for differentiation between groups whether stifles were clipped or not. Early accurate thermographic detection of stifle diseases may be possible as technology improves.

MRI

MRI detects emitted radiofrequency (RF) signals that are converted into a computerized gray-scale image or tomogram. In the 1970s, the concept of magnetic field gradients whereby an image based on magnetic resonance could be produced ushered in a new method of medical imaging.[1,50] The major advantages of MRI are its excellent image resolution, superior soft tissue contrast, acquisition of images in any plane, and use of a magnetic field rather than ionizing radiation. Because protons in different tissues realign at different rates, the RF signal received by the RF coil can be filtered to accentuate different tissue characteristics using specific "sequences." Additionally, contrast agents can be directly injected into a joint (MR arthrograms). With the introduction of region specific surface coils and stronger magnets, improved signal-to-noise ratio (SNR), enhanced spatial resolution and abbreviated scan times, MRI is now commonly used in people to assess internal derangements of the knee, wrist, hip, hand, and shoulder.[50–54]

OA is most commonly assessed using radiography in both people and animals.[4,6,55–57] Several reports describe successful use of MRI for documentation and quantification of OA in dogs with naturally occurring and experimental models of CCL deficient stifles. [7,58–62] MRI superior is superior to radiography for detection of early OA in a canine experimental model.[63] When applying MRI to the musculoskeletal system, the imaging plane and pulse sequences are dependent on the structures being imaged. Because the stifle is a complex joint with various tissue types, differing image planes and sequences are typically used for complete evaluation (Fig 5).

Healthy articular cartilage has intermediate signal intensity on TI- and T2-weighted images, and high signal intensity on a fat suppressed turbospin echo sequence. Substances that consistently have high signal intensity on the T1-weighted images include fat and contrast. Synovial fluid and edema have high-signal intensity on T2-weighted sequences and low signal on TI-weighted sequences. The signal intensity from cortical bone, tendons, ligaments, and menisci is weak because they are not naturally hydrated tissues and therefore lack mobile protons.

CCL rupture is the most common cause of stifle OA in dogs and is frequently associated with damage to the medial meniscus.[4,64–66] Complete evaluation of the menisci is impossible even with arthrotomy or arthroscopy because of anatomic constraints. Using either technique, the tibial surface of the menisci remains hidden from view, as does the integrity of internal meniscal structure.[66–68] Additional meniscal surgery after surgical stabilization for CCL deficient stifle joints may be needed because of undiagnosed meniscal pathology at the time of the initial surgery.[69] MRI evaluation of the internal architecture of the stifle joint affords many advantages over arthroscopy or arthrotomy and is the primary imaging modality when assessing for cruciate, meniscal, and articular pathology in people.[50–52] Because dedicated surface coils for animals are not readily available, using an MR coil that closely approximates the size and configuration of the joint being imaged will improve the SNR and thus image quality.[50–52]

The advantages of using a low-field system must be weighed against the substantial decrease in resolution often essential to accurate image interpretation. Meniscal grading scales used in assessing people have not correlated well to findings in dogs imaged with low-field (0.3 T) MRI techniques; however, results were superior to those of

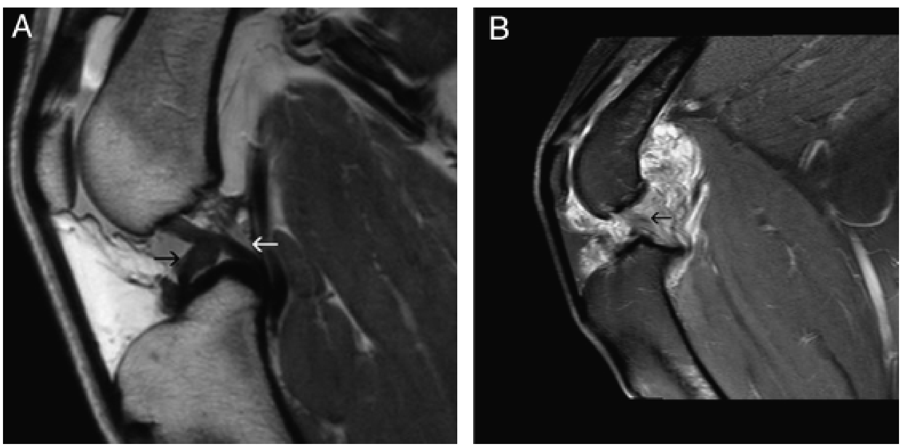

Figure 5 (A) T1 turbo spin echo (TSE) sagittal magnetic resonance imaging (MRI) of a normal stifle joint. Cranial cruciate ligament (black arrow), caudal cruciate ligament (white arrow). (TR/TE = 2265/14, slice thickness = 1.5, 0 gap, FOV = 12, matrix = 284 × 240), Philips Achieva 3.0 T (Philips, Andover, MA). (B) Proton density TSE spectral attenuated inversion recovery sagittal MRI of a stifle joint with degenerative joint disease. The caudal cruciate ligament (black arrow) is evident within the joint. Stifle effusion is seen as a mixed hyperintensity within the joint. (TR/TE = 3368/30, slice thickness = 2, 0 gap, FOV = 14, matrix = 284 × 200), Philips Achieva 3.0 T.

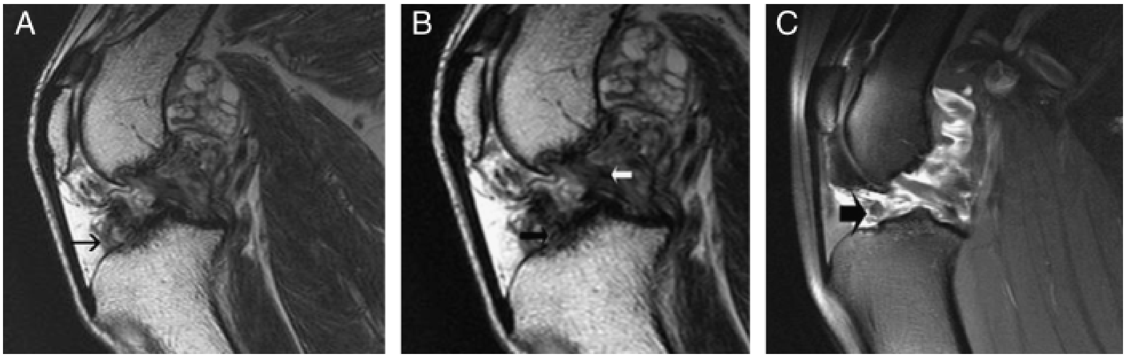

Figure 6 (A) Proton density sagittal magnetic resonance imaging (MRI) of a stifle showing a cranial lateral meniscal tear (black arrow). (TR/TE = 1699/14, slice thickness = 2, 0 gap, FOV = 13, matrix = 264 × 240), Philips Achieva 3.0 T. (B) A T2 turbo spin echo sagittal oblique MRI of a stifle with a cranial cruciate ligament (CCL) rupture (black arrow). There is mixed hyperintensity of the caudal cruciate ligament indicating thickening (open black arrow). (TR/TE 3000/100, slice thickness = 1.2, 0.1 gap, FOV = 11, matrix = 248 × 192), Philips Achieva 3.0 T. (C) MR arthrogram showing CCL rupture (black arrow) using a T1 FATSAT sagittal sequence. (TR/TE = 596/20, slice thickness = 1.7, 0.2 gap, FOV = 11, matrix = 332 × 234), Philips Achieva 3.0 T.

arthroscopy.[70] Increased magnet strength may provide the resolution needed to appreciate the earlier stages of meniscal degeneration thought to precede grade 3 or grade 4 tears, which are not readily seen on low-field MRI scans. Equally important is the prolonged scan times associated with low field magnets, often resulting in the doubling or tripling scan times of high-field systems.

In dogs, abnormal signal intensity with thickening of the CCL found with stifle MRI is associated with partial CCL rupture whereas an inability to image the CCL with the presence of previously described MRI degenerative changes is found with complete CCL rupture. The aforementioned MRI findings are more readily observed using an MR arthrography technique.[59]

The evaluation of meniscal integrity is also enhanced using a combination of sagittal and dorsal images and MR arthrography.[59] If joint effusion is present, observation of intraarticular structures is improved on T2-weighted images without administering intraarticular contrast, known as the "arthrogram effect"(Fig 6).[71] Intravenous contrast does not permit contrast enhancement sufficient in the imaging time frame allotted, when compared with intraarticular administration. Additionally, no negative effects associated with intraarticular contrast use have been reported in dogs and only rare reactions occur in people.[72,73] For MR arthrography in dogs with CCL deficient stifles, T1-weighted conventional spin echo images and T2-weighted fat-suppressed fast spin echo images are recommended to maximize contrast between the gadolinium in the joint and the menisci and capsular ligaments.[59] Sequence details are often magnet size and coil specific, therefore the results of specific protocols may vary between imaging centers.

Subchondral cyst-like lesions, bone bruises, geodes, and high-signal intensity short-tau inversion recovery (STIR) lesions are terms used to describe ill defined signal intensities seen as abnormalities on articular MRI scans.[74–77] Signal alterations seen in the subchondral bone marrow of the distal aspect of the femur and proximal aspect of the tibia are common findings in people with traumatic cruciate ligament injuries and OA and are referred to as a "bone bruises."[78,79] There is evidence that an MRI finding of a bone bruise can be induced with an experimental trauma in dogs.[80,81] These injuries are associated with marked histologic and biochemical changes despite grossly normal articular cartilage, thus providing support to the theory that progressive degenerative joint disease may contribute to ligamentous deterioration and precede actual ligament rupture in clinical cases of CCL rupture in dogs. In both clinical cases and in experimental models of CCL rupture in dogs, the location of the MRI lesions is typically the intercondylar fossa of the femur and in the intercondylar eminence of the tibia (Fig 7). This is thought to be in part related to abnormal stresses born by the remaining caudal cruciate ligament and subsequent sequela in the cancellous bone subchondral region associated with its origin and insertion.[70,77,82] Early detection of theoretical pre-CCL rupture lesions by stifle MRI evaluation may afford clinicians an early opportunity to intervene medically before subsequent CCL rupture.

Bone neoplastic processes have been assessed in people including those of the appendicular skeletal system for purpose of limb sparing procedures.[83,84] Using a combination of T1-weighted, T2-weighted and STIR sequences is useful when considering the variety of cortical and bone marrow alterations to be identified. There is a paucity of information in the veterinary literature about sue of MRI versus CT scan and conventional radiography for identification and determination of the extent of neoplastic disease for prognostic and surgical planning purposes. In a comparison of the accuracy of the 3 modalities in 10 amputated limbs, measurements made by each were fairly accurate in predicting tumor length. It was considered by the authors, however, to be advantageous to use additional imaging studies to confirm the extent of neoplastic disease because some evidence of underestimation (radiography and CT) and overestimation (MRI) was observed (Fig 8).[85] The trend toward increased magnet strength ($\geq$3.0 T) to improve SNR has continued in human medicine despite

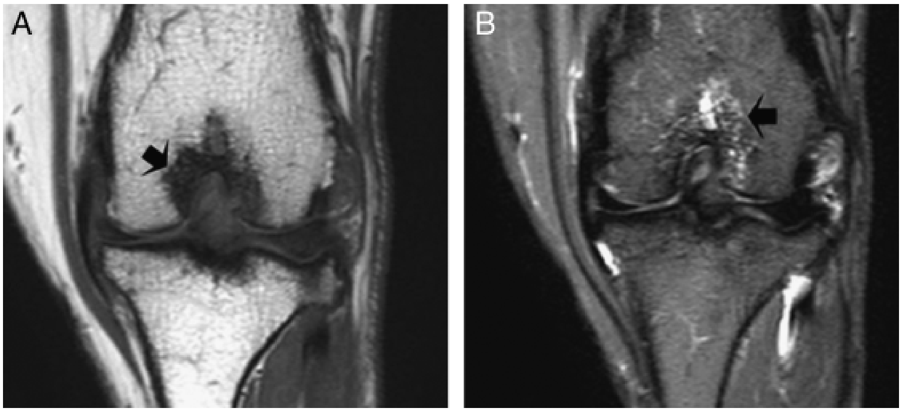

Figure 7 (A) T1 turbo spin echo dorsal magnetic resonance imaging (MRI) of a femoral intercondylar notch bone bruise (black arrow). (TR/TE = 581/20, slice thickness = 1.7, 0.5 gap, FOV = 12, matrix = 308 × 252). (B) Short-tau inversion recovery dorsal MRI of a femoral intercondylar notch bone bruise (black arrow). *Caudal cruciate ligament (TR/TE = 3967/30, TI = 190, slice thickness = 2, 0.2 gap, FOV = 12, matrix = 292 × 216), Philips Achieva 3.0 T.

increased purchase, cryogen and maintenance costs, because of the superior resolution and shorter scan times.[83] Because the anatomic structures being imaged are dogs and cats than found in people, the benefits of improved resolution become indispensable.

CT

CT is based on tomography technology developed in the early 1900s which allowed for an image of a single slice of the body to be produced on radiographic film. Images can be manipulated, with a computerized process known as windowing, to reveal various structures based on tissue characteristics. With recent advances, modern scanners allow this data to be reformatted as volumetric (3D) representations of structures. From this, a 3D model can be constructed and displayed. Multiple models can be constructed from various thresholds, allowing different colors to represent each anatomic component (bone, muscle, cartilage; Fig 9). Clinical advantages of using multidetector helical CT scanners include improved patient safety, enhanced accuracy and most strikingly, the ability to perform 3D image reconstructions with the option of creating surgical models to plan surgery for complex cases. We are unaware of reports of the use of CT for assessment of canine degenerative joint disease; however, a scale characterizing the severity of degenerative joint disease was included as part of a recent report on the use of CT arthrography (CTA) in assessing canine stifles.

Despite the common finding of osteochondritis dissecans (OCD) in dogs[86–88] there is only 1 report of the use of CT for diagnosis of OCD.[89] CT evaluation of the intercondylar notch of canine stifles can be easily obtained and

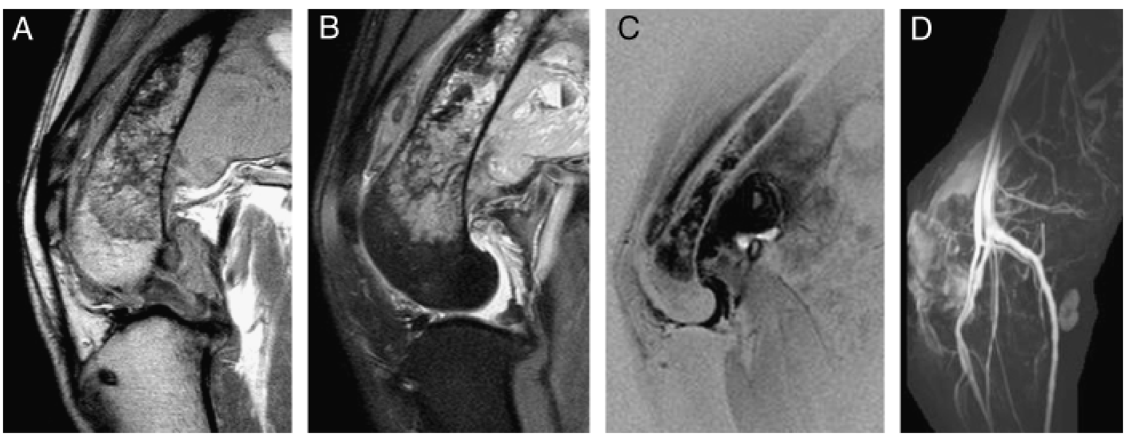

Figure 8 Magnetic resonance series of a distal femoral osteosarcoma. (A) T1-weighted proton density (PD) sagittal magnetic resonance imaging (MRI). The tumor is seen as a mixed hypointensity of the distal medullary canal. (TR/TE = 1974/14, slice thickness = 1.5, 0 gap, FOV = 12, matrix = 284 × 240), Philips Achieva 3.0 T. (B) PD spectral attenuated inversion recovery sagittal MRI. The medullary canal is a mixed hyperintensity (TR/TE = 5918/30, slice thickness = 1.5, 0 gap, FOV = 12, matrix = 268 × 210), Philips Achieva 3.0 T. (C) Inverted short-tau inversion recovery sagittal MRI showing the extent of the tumor. (D) T1 fast field echo contrast-enhanced MR arthrography of the stifle highlighting the increased blood supply to the osteosarcoma.

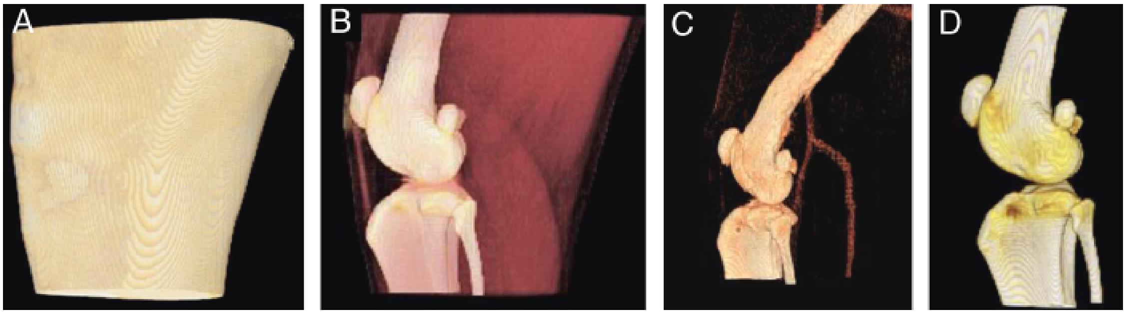

Figure 9 Three-dimensional stifle computed tomographic scan with reconstruction by tissue layer; (A) skin, (B) muscle, (C) vascular, (D) bone.

more reliable when compared with conventional radiographs.[90,91] Additionally, the superior image quality is attributed to the avoidance of osseous or soft tissue superimposition.[90] The modality of choice for imaging the human knee is MRI; however, CTA has been reported to have similar sensitivity and specificity to MRI for detection of meniscal injury.[92] Successful identification of intraarticular structures has been reported with CTA in normal[93] and cadaveric canine stifles.[94,95] Care during administration of intraarticular contrast to avoid the fat pad and a concentration of 150 mg iodine/mL is recommended to enhance visualization without contrast obscuring structures because of excessive bloom.[93] Removal of a small amount of joint fluid, especially in dogs with severe joint effusion, and flexing and extending the joint gently has been recommended to enhance contrast dispersion.[93–96]

In a recent report of CTA to assess intraarticular structures in dogs with naturally occurring stifle ligamentous dysfunction, sensitivities and specificities were 96–100% and 75–100% respectively for the identification of CCL rupture.[96] In the same report; however, reviewers were less adept at discriminating torn meniscal fibrocartilage, with sensitivities of 13.3–73.3% and specificities of 57.1–100%. Because use of CTA in assessing canine stifles (Fig 10) remains in its infancy, reviewers were all ''inexperienced'' in assessing stifle pathology using this modality which undoubtedly contributed to the differences reported compared with the human literature.

A pilot study of pre- and postoperative evaluations of dogs with medial patellar luxations using CT technology did find CT useful in documenting the effects of surgery (medial releasing desmotomy, lateral imbrication, modification of the femoral trochlear groove and tibial crest transposition) on the stifle.[97] In that study, restoration of the quadriceps apparatus and adequate deepening of the femoral trochlear groove were successfully achieved. Additionally noted was caudalization of the patellar tendon and lateralization of the tibial tuberosity, the clinical significance of which remains undetermined.

There are several reports describing use of CT for detection of neoplastic disease in animals for prognostic and surgical planning purposes. The assessment of CT in 10 amputated limbs, revealed CT was fairly accurate in predicting tumor length (Fig 11); however, it was considered to be advantageous to use additional imaging studies to confirm the extent of neoplastic disease because some evidence of underestimation was observed.[85] Although CT scanners have been used frequently in human medicine to assess intraarticular structures and have the benefit of providing better osseous visualization and shorter scan times when compared with MRI[105,106] most stifle imaging studies in veterinary medicine are centered on the assessment of intraarticular ligamentous abnormalities making MRI a more suitable modality.

The canine stifle represents a diagnostic challenge because of its complex composition. MRI has recently been defined as the ''gold standard'' in human medicine because of the flexibility it affords the clinician when faced with imaging several different tissue types in a single structure. Thermal imaging offers the advantage of objectively

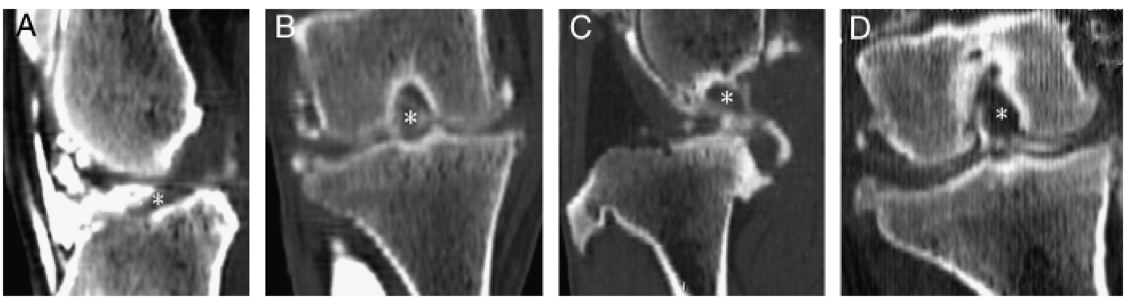

Figure 10 Sagittal (A) and dorsal (B) computed tomographic arthrography (CTA) images of a normal canine stifle, *cranial cruciate ligament (CCL), caudal cruciate ligament (black arrow) and sagittal (C), and dorsal (D) CTA images of a CCL-deficient stifle; only the *caudal cruciate ligament is visible.

Figure 11 Sagittal computed tomographic image of distal femoral osteosarcoma. Note the periosteal reaction (solid black arrow) along the femur, and bone lysis (open black arrow) in the medullary canal.

viewing physiologic changes within the anatomic region of interest before the onset of structural change. Regardless of the imaging modality, progress in computing technology has accelerated advances in diagnostic imaging. The key to successful management of the diagnostic options available is to have a thorough understanding of the anatomy and tissue properties of region being imaged and to recognize the strengths and weaknesses of the modality being selected. Ultimately, a multimodality approach will likely provide a complete assessment of complex structures using the strengths of each modality to exploit the tissue characteristics of the structure being imaged.

REFERENCES

1. Buschong S: *Magnetic Resonance Imaging* (ed 2). St. Louis, MO, Mosby-Year Book, 1996
2. Thrall DE: *Textbook of Veterinary Diagnostic Radiology* (ed 4). Philadelphia, PA, W. B. Saunders, 2002
3. Kealy JK, McAllister H: *Diagnostic Radiology and Ultrasonography of the Dog and Cat* (ed 3). Philadelphia, PA, W. B. Saunders, 2000
4. Carrig CB: Diagnostic imaging of osteoarthritis. *Vet Clin North Am Small Anim Pract* 1997;27:777–814
5. Burk RL, Ackerman N: *Small Animal Radiology and Ultrasonography* (ed 2). Philadelphia, PA, W. B. Saunders, 1996
6. Innes JF, Costello M, Barr FJ, et al: Radiographic progression of osteoarthritis of the canine stifle joint: a prospective study. *Vet Radiol Ultrasound* 2004;45:143–148
7. D'Anjou MA, Moreau M, Troncy E, et al: Osteophytosis, subchondral bone sclerosis, joint effusion and soft tissue thickening in canine experimental stifle osteoarthritis: comparison between 1.5 T magnetic resonance imaging and computed radiography. *Vet Surg* 2008;37:166–177
8. Whatmough C, Moores AP, Magalhaes RS, et al: Factors affecting width of the canine femorotibial joint space in nonweight-bearing radiographs. *Vet Radiol Ultrasound* 2008;49:129–134
9. De Rooster H, Van Bree H: Use of compression stress radiography for the detection of partial tears of the canine cranial cruciate ligament. *J Small Anim Pract* 1999;40:573–576
10. De Rooster H, Van Ryssen B, Van Bree H: Diagnosis of cranial cruciate ligament injury in dogs by tibial compression radiography. *Vet Rec* 1998;142:366–368
11. de Rooster H, van Bree H: Radiographic measurement of craniocaudal instability in stifle joints of clinically normal dogs and dogs with injury of a cranial cruciate ligament. *Am J Vet Res* 1999;60:1567–1570
12. de Bruin T, de Rooster H, Bosmans T, et al: Radiographic assessment of the progression of osteoarthrosis in the contralateral stifle joint of dogs with a ruptured cranial cruciate ligament. *Vet Rec* 2007;161:745–750
13. Dudley RM, Kowaleski MP, Drost WT, et al: Radiographic and computed tomographic determination of femoral varus and torsion in the dog. *Vet Radiol Ultrasound* 2006;47:546–552
14. Mostafa AA, Griffon DJ, Thomas MW, et al: Proximodistal alignment of the canine patella: radiographic evaluation and association with medial and lateral patellar luxation. *Vet Surg* 2008;37:201–211
15. Langley-Hobbs SJ, Brown G, Matis U: Traumatic fracture of the patella in 11 cats. *Vet Comp Orthop Traumatol* 2008;21:427–433
16. Guillaumot P, Scotti S, Carozzo C, et al: Two cases of surgically treated feline patellar fractures. *Vet Comp Orthop Traumatol* 2008;21:156–158
17. Mattern KL, Berry CR, Peck JN, et al: Radiographic and ultrasonographic evaluation of the patella ligament following tibial plateau leveling osteotomy. *Vet Radiol Ultrasound* 2006;47:185–191
18. Shipov A, Shahar R, Joseph R, et al: Successful management of bilateral patellar tendon rupture in a dog. *Vet Comp Orthop Traumatol* 2008;21:181–184
19. Kippenes H, Johnston G: Diagnostic imaging of osteochondrosis. *Vet Clin North Am Small Anim Pract* 1998;28:137–160
20. Fitch RB, Wilson ER, Hathcock JT, et al: Radiographic, computed tomographic and magnetic resonance imaging evaluation of a chronic long digital extensor tendon avulsion in a dog. *Vet Radiol Ultrasound* 1997;38:177–181
21. Reed AL, Payne JT, Constantinescu GM: Ultrasonographic anatomy of the normal canine stifle. *Vet Radiol Ultrasound* 1995;36:315–321
22. Kramer M, Stengel H, Gerwing M, et al: Sonography of the canine stifle. *Vet Radiol Ultrasound* 1999;40:282–293
23. Seong Y, Eom K, Lee H, et al: Ultrasonographic evaluation of cranial cruciate ligament rupture via dynamic intra-articular saline injection. *Vet Radiol Ultrasound* 2005;46: 80–82

24. Mahn MM, Cook JL, Cook CR, et al: Arthroscopic verification of ultrasonographic diagnosis of meniscal pathology in dogs. *Vet Surg* 2005;34:318–323
25. Peter L: *Meditherm Manual of Clinical Thermology*. Beaufort, Meditherm Inc., 2004
26. Loughin CA, Marino DJ: Evaluation of thermographic imaging of the limbs of healthy dogs. *Am J Vet Res* 2007;68:1064–1069
27. Peter L: *Manual of Equine Thermography*. Beaufort, Meditherm, Inc., 2002
28. Eddy AL, Van Hoogmoed LM, Snyder JR: The role of thermography in the management of equine lameness. *Vet J* 2001;162:172–181
29. Turner TA: Diagnostic thermography. *Vet Clin North Am Equine Pract* 2001;17:95–113
30. Purohit RC, McCoy MD: Thermography in the diagnosis of inflammatory processes in the horse. *Am J Vet Res* 1980;41: 1167–1174
31. Vaden MF, Purohit RC, McCoy MD, et al: Thermography: a technique for subclinical diagnosis of osteoarthritis. *Am J Vet Res* 1980;41:1175–1179
32. Ring EF, Dieppe PA, Bacon PA: The thermographic assessment of inflammation and anti-inflammatory drugs in osteoarthritis. *Br J Clin Pract* 1981;35:263–264
33. Um SW KM, Lim JH, et al: Thermographic evaluation for the efficacy of acupuncture on induced chronic arthritis in the dog. *J Vet Med Sci* 2005;67:1283–1284
34. Dobi I, Kekesi V, Toth M, et al: Endothelin-induced long-lasting mesenteric vasoconstriction: a hypothetical mechanism of non-occlusive intestinal infarction. *Acta Chir Hung* 1991;32:199–208
35. Adachi H, Becker LC, Ambrosio G, et al: Assessment of myocardial blood flow by real-time infrared imaging. *J Surg Res* 1987;43:94–102
36. Daniel W, Klein H, Hetzer R, et al: Thermocardiography—a method for continuous assessment of myocardial perfusion dynamics in the exposed animal and human heart. *Thorac Cardiovasc Surg* 1979;27:51–57
37. Stein LE, Pijanowski GJ, Johnson AL, et al: A comparison of steady state and transient thermography techniques using a healing tendon model. *Vet Surg* 1988;17:90–96
38. Vujcic M, Nedeljkovic R: Thermography in the detection and follow up of chondromalacia patellae. *Ann Rheum Dis* 1991; 50:921–925
39. Devereaux MD, Parr GR, Lachmann SM, et al: Thermographic diagnosis in athletes with patellofemoral arthralgia. *J Bone Joint Surg Br* 1986;68:42–44
40. Salisbury RS, Parr G, De Silva M, et al: Heat distribution over normal and abnormal joints: thermal pattern and quantification. *Ann Rheum Dis* 1983;42:494–499
41. Collins AJ, Ring F, Bacon PA, et al: Thermography and radiology complimentary methods for the study of inflammatory diseases. *Clin Radiol* 1976;27:237–243
42. Rajapakse C, Grennan DM, Jones C, et al: Thermography in the assessment of peripheral joint inflammation—a re-evaluation. *Rheumatol Rehabil* 1981;20:81–87
43. Ring EF: Thermographic and scintigraphic examination of the early phase of inflammatory disease. *Scand J Rheumatol Suppl* 1987;65:77–80
44. DeSilva M, Kyle V, Hazleman B, et al: Assessment of inflammation in the rheumatoid knee joint: correlation between clinical, radioisotopic, and thermographic methods. *Ann Rheum Dis* 1986;45:277–280
45. Goldie I: Is thermography more than an adjuvant in orthopedic diagnostics? *Orthopedics* 1985;8:1128–1129
46. Siegel MG, Siqueland KA, Noyes FR: The use of computerized thermography in the evaluation of non-traumatic anterior knee pain. *Orthopedics* 1987;10:825–830
47. Varju G, Pieper CF, Renner JB, et al: Assessment of hand osteoarthritis: correlation between thermographic and radiographic methods. *Rheumatology (Oxford)* 2004;43: 915–919
48. Marr CM: Microwave thermography: a non-invasive technique for investigation of injury of the superficial digital flexor tendon in the horse. *Equine Vet J* 1992;24:269–273
49. Mangine RE, Siqueland KA, Noyes FR: The use of thermography for the diagnosis and management of patellar tendinitis. *J Orthop Sports Phys Ther* 1987;9:132–140
50. Berquist T, Ehman RL, Richardson ML, eds: *Magnetic Resonance Imaging of the Musculoskeletal System* (ed 2). New York, NY, Raven Press, 1990
51. Harms S, Greenway G: *Musculoskeletal System*. St. Louis, MO, Mosby, 1988, pp 1323–1433
52. Moon KL Jr., Genant HK, Helms CA, et al: Musculoskeletal applications of nuclear magnetic resonance. *Radiology* 1983;147:161–171
53. Stoller D: *Magnetic Resonance Imaging in Orthopaedics and Rheumatology*, in. Philadelphia, PA, Lippincott, 1989, pp 1–284
54. Burk DL Jr., Dalinka MK, Schiebler ML, et al: Strategies for musculoskeletal magnetic resonance imaging. *Radiol Clin North Am* 1988;26:653–672
55. Peterfy C, Kothari M: Imaging osteoarthritis: magnetic resonance imaging versus x-ray. *Curr Rheumatol Rep* 2006;8:16–21
56. Raynauld JP, Martel-Pelletier J, Berthiaume MJ, et al: Long term evaluation of disease progression through the quantitative magnetic resonance imaging of symptomatic knee osteoarthritis patients: correlation with clinical symptoms and radiographic changes. *Arthritis Res Ther* 2006;8:R21
57. Raynauld JP, Martel-Pelletier J, Berthiaume MJ, et al: Quantitative magnetic resonance imaging evaluation of knee osteoarthritis progression over two years and correlation with clinical symptoms and radiologic changes. *Arthritis Rheum* 2004;50:476–487
58. Widmer WR, Buckwalter KA, Braunstein EM, et al: Radiographic and magnetic resonance imaging of the stifle joint in experimental osteoarthritis of dogs. *Vet Radiol Ultrasound* 1994;35:371–383
59. Banfield CM, Morrison WB: Magnetic resonance arthrography of the canine stifle joint: technique and applications in eleven military dogs. *Vet Radiol Ultrasound* 2000;41:200–213

60. Martig S, Boisclair J, Konar M, et al: MRI characteristics and histology of bone marrow lesions in dogs with experimentally induced osteoarthritis. *Vet Radiol Ultrasound* 2007;48: 105–112
61. Sabiston CP, Adams ME, Li DK: Magnetic resonance imaging of osteoarthritis: correlation with gross pathology using an experimental model. *J Orthop Res* 1987;5:164–172
62. Libicher M, Ivancic M, Hoffmann M, et al: Early changes in experimental osteoarthritis using the Pond-Nuki dog model: technical procedure and initial results of in vivo MR imaging. *Eur Radiol* 2005;15:390–394
63. Nolte-Ernsting CC, Adam G, Buhne M, et al: MRI of degenerative bone marrow lesions in experimental osteoarthritis of canine knee joints. *Skeletal Radiol* 1996;25:413–420
64. Hulse D, Shires PK: Observation of the posteromedial compartment of the stifle joint.. *J Am Anim Hosp Assoc* 1981;17:575–578
65. Bennett D, May C: Meniscal damage associated with cruciate disease in the dog. *J Small Anim Pract* 1991;32:111–117
66. Flo GL: Meniscal injuries. *Vet Clin North Am Small Anim Pract* 1993;23:831–843
67. Anderson MW: MR imaging of the meniscus. *Radiol Clin North Am* 2002;40:1081–1094
68. Jackson J VP, Griffey S, Walls CM, et al: Pathologic changes in grossly normal menisci in dogs with rupture of the cranial cruciate ligament. *J Am Vet Med Assoc* 2001;218:1281–1284
69. Metelman L, Schwarz PD, Salman M, et al: An evaluation of three different cranial cruciate ligament surgical stabilization procedures as they relate to postoperative meniscal injuries. *Vet Comp Orthop Traumatol* 1995;8:118–123
70. Martig S, Konar M, Schmokel HG, et al: Low-field MRI and arthroscopy of meniscal lesions in ten dogs with experimentally induced cranial cruciate ligament insufficiency. *Vet Radiol Ultrasound* 2006;47:515–522
71. Helgason JW, Chandnani VP, Yu JS: MR arthrography: a review of current technique and applications. *Am J Roentgenol* 1997;168:1473–1480
72. Newberg AH, Munn CS, Robbins AH: Complications of arthrography. *Radiology* 1985;155:605–606
73. Hajek PC, Sartoris DJ, Gylys-Morin V, et al: The effect of intra-articular gadolinium-DTPA on synovial membrane and cartilage. *Invest Radiol* 1990;25:179–183
74. Eggers GWN, Evans EB, Butler JK, Blumer J: The pathogenesis, significance and treatment of subchondral cysts of the iliac acetabulum. *J Bone and Joint Surg Am* 1959;766
75. Resnick D NG: Degenerative disease of extraspinal locations, in Resnick D NG (ed): *Diagnosis of Bone and Joint Disorders*. Philadelphia, PA, W. B. Saunders, 1988, pp 1271–1278
76. Moore EA, Jacoby RK, Ellis RE, et al: Demonstration of a geode by magnetic resonance imaging: a new light on the cause of juxta-articular bone cysts in rheumatoid arthritis. *Ann Rheum Dis* 1990;49:785–787
77. Winegardner KR, Scrivani PV, Krotscheck U, et al: Magnetic resonance imaging of subarticular bone marrow lesions in dogs with stifle lameness. *Vet Radiol Ultrasound* 2007;48: 312–317
78. Rosen MA, Jackson DW, Berger PE: Occult osseous lesions documented by magnetic resonance imaging associated with anterior cruciate ligament ruptures. *Arthroscopy* 1991;7:45–51
79. Newberg AH, Wetzner SM: Bone bruises: their patterns and significance. *Semin Ultrasound CT MR* 1994;15:396–409
80. Donohue JM, Buss D, Oegema TR Jr., et al: The effects of indirect blunt trauma on adult canine articular cartilage. *J Bone Joint Surg Am* 1983;65:948–957
81. Mrosek EH, Lahm A, Erggelet C, et al: Subchondral bone trauma causes cartilage matrix degeneration: an immunohistochemical analysis in a canine model. *Osteoarthritis Cartilage* 2006;14:171–178
82. Baird DK, Hathcock JT, Kincaid SA, et al: Low-field magnetic resonance imaging of early subchondral cyst-like lesions in induced cranial cruciate ligament deficient dogs. *Vet Radiol Ultrasound* 1998;39:167–173
83. Van der Woude H BJ, Pope T: Magnetic resonance imaging of the musculoskeletal system. *Clin Orthop* 1998;347:272–286
84. O'Flanagan SJ, Stack JP, McGee HM, et al: Imaging of intramedullary tumour spread in osteosarcoma. A comparison of techniques. *J Bone Joint Surg Br* 1991;73: 998–1001
85. Davis GJ, Kapatkin AS, Craig LE, et al: Comparison of radiography, computed tomography, and magnetic resonance imaging for evaluation of appendicular osteosarcoma in dogs. *J Am Vet Med Assoc* 2002;220:1171–1176
86. Denny HR, Gibbs C: Osteochondritis dissecans of the canine stifle joint. *J Small Anim Pract* 1980;21:317–322
87. Alexander J, Richardson DC, Secler BA: Osteochondritis dissecans of the elbow, stifle, and hock—a review. *J Am Anim Hosp Assoc* 1981;17:51–56
88. Montgomery R, Milton JL, Henderson RA: Osteochondritis of the canine stifle. *Compend Cont Educ Pract Vet* 1989;11: 1199–1205
89. Kulendra E, Lee K, Schoeniger S, et al: Osteochondritis dissecans-like lesion of the intercondylar fossa of the femur in a dog. *Vet Comp Orthop Traumatol* 2008;21:152–155
90. Fitch RB, Hathcock JT, Montgomery RD: Radiographic and computed tomographic evaluation of the canine intercondylar fossa in normal stifles and after notchplasty in stable and unstable stifles. *Vet Radiol Ultrasound* 1996;37: 266–274
91. Lewis BA, Allen DA, Henrikson TD, et al: Computed tomographic evaluation of the canine intercondylar notch in normal and cruciate deficient stifles. *Vet Comp Orthop Traumatol* 2008;21:119–124
92. Vande Berg BC, Lecouvet FE, Poilvache P, et al: Anterior cruciate ligament tears and associated meniscal lesions: assessment at dual-detector spiral CT arthrography. *Radiology* 2002;223:403–409
93. Samii VF, Dyce J: Computed tomographic arthrography of the normal canine stifle. *Vet Radiol Ultrasound* 2004;45: 402–406
94. Tivers MS, Mahoney P, Corr SA: Canine stifle positive contrast computed tomography arthrography for assessment of caudal horn meniscal injury: a cadaver study. *Vet Surg* 2008;37:269–277

95. Han S, Cheon H, Cho H, et al: Evaluation of partial cranial cruciate ligament rupture with positive contrast computed tomographic arthrography in dogs. *J Vet Sci* 2008;9:395–400

96. Samii VF, Dyce J, Pozzi A, et al: Computed tomographic arthrography of the stifle for detection of cranial and caudal cruciate ligament and meniscal tears in dogs. *Vet Radiol Ultrasound* 2009;50:144–150

97. Towle HA, Griffon DJ, Thomas MW, et al: Pre- and postoperative radiographic and computed tomographic evaluation of dogs with medial patellar luxation. *Vet Surg* 2005;34:265–272